

Excited levels in ^{145}Pm

W. Urban, T. Rząca-Urban,* J. L. Durell, Ch. P. Hess, C. J. Pearson, W. R. Phillips, B. J. Varley, and W. J. Vermeer
Department of Physics and Astronomy, University of Manchester, Manchester M13 9PL, United Kingdom

Ch. Vieu and J. S. Dionisio
Centre de Spectrometrie Nucléaire et Spectrometrie de Masse, 91405 Orsay, France

M. Pautrat
Institut de Physique Nucléaire, Boîte Postale No. 1, 91406 Orsay, France

J. C. Bacelar
Kernfysisch Versneller Instituut, University of Groningen, NL-9747 AA Groningen, The Netherlands
 (Received 22 May 1996)

High-spin states in ^{145}Pm have been studied with TESSA3 operating at NSF Daresbury, through the $^{134}\text{Xe}(^{15}\text{N},4n)$ compound nucleus reaction using a solid xenon target. To determine conversion coefficients and properties of low-spin excitations electron- γ and γ - γ coincidences have been measured following the $^{146}\text{Nd}(d,3n)$ reaction. An extended level scheme of ^{145}Pm is proposed and interpreted in terms of single-particle excitations with collective quadrupole and octupole vibrations coupled to them. [S0556-2813(96)02711-2]

PACS number(s): 21.10.Re, 21.10.Pc, 23.20.Lv, 27.60.+j

I. INTRODUCTION

The nucleus ^{145}Pm has a pair of valence neutrons and three proton holes with respect to the doubly closed shell nucleus ^{146}Gd . Therefore one may expect that its excitation pattern will be dominated by single-particle configurations and vibrationlike, collective excitations. Pronounced octupole excitations observed in the neighboring nuclei (like ^{149}Tb [1]) suggest that octupole collectivity may play an important role in the excitation mechanism of ^{145}Pm . Early studies of ^{145}Pm [2–5], using low angular momentum (p,xn) and ($^3\text{He},d$) reactions, provided detailed knowledge of low-spin excitations, interpreted [5] within the cluster-vibration model (CVM). However, those reactions did not produce enough angular momentum to study octupole excitations. Recent high-spin works [6,7] produced excited levels up to spin $I = \frac{33}{2}$ using the ($^{19}\text{F},4n$) reaction. Many states of both parities have been reported but the presence of octupole excitations has not been discussed. Moreover, the interpretation of some of the excited levels in ^{145}Pm given in Refs. [6,7] is inconsistent with the systematics [1,8]. For all these reasons, we performed studies of medium-to-high-spin excitations in the nucleus ^{145}Pm , using $^{146}\text{Nd}+d$ and $^{134}\text{Xe}+^{15}\text{N}$ compound nucleus reactions. Special attention has been paid to octupole-phonon excitations but we also reinterpreted many of the multiparticle configurations observed in ^{145}Pm . This study is part of our systematic search for the octupole effect in promethium nuclei [9–12].

The contents of this work are following. Experimental methods used in this investigations are discussed in Sec. II. The analysis of the data and the corresponding results are

reported in Sec. III. The buildup of the nuclear level scheme of ^{145}Pm is described in Sec. IV which is followed by interpretation of the results, presented in Sec. V.

II. EXPERIMENTAL METHODS

A. $^{134}\text{Xe}(^{15}\text{N},xn)$ reaction

Medium-to-high spins in ^{145}Pm were studied in the $^{134}\text{Xe}+^{15}\text{N}$ compound nucleus reaction using the 78 MeV ^{15}N beam delivered by the NSF Daresbury. A target of solidified xenon on a Pb backing has been used for a double purpose: (i) reduction of the Doppler broadening of γ rays emitted by recoil nuclei and (ii) high production rate of ^{145}Pm by increasing target density (for more details see Ref. [13]). The Xe material used consisted of 90% of ^{136}Xe , 8% of ^{134}Xe , and 2% of lighter Xe isotopes. With the total thickness of frozen Xe of about 3 mg/cm^2 , the partial thickness for the ^{134}Xe isotope was about $250\text{ }\mu\text{g/cm}^2$. The γ - γ coincidences were measured using the TESSA3 spectrometer, which consisted of 16 Compton-suppressed Ge detectors and a γ -multiplicity and sum-energy filter. Four detectors were placed at 90° and eight at 35° with respect to the beam direction, which provided the possibility to measure directional correlations of γ rays (DCO ratios). Coincidence events consisting of two γ -energy signals, a γ - γ time, and a multiplicity signal were recorded. A total amount of 2.2×10^7 coincidence events were collected, with about 2×10^6 events corresponding to the $^{134}\text{Xe}(^{15}\text{N},4n)^{145}\text{Pm}$ channel.

B. $^{146}\text{Nd}(d,xn)$ reaction

To investigate in detail the low excited levels of ^{145}Pm and to find their parities, an internal conversion measurement has been performed at the MP tandem accelerator at Orsay,

*Permanent address: Institute of Experimental Physics, Warsaw University, ul. Hoza 69, 00681 Warsaw, Poland.

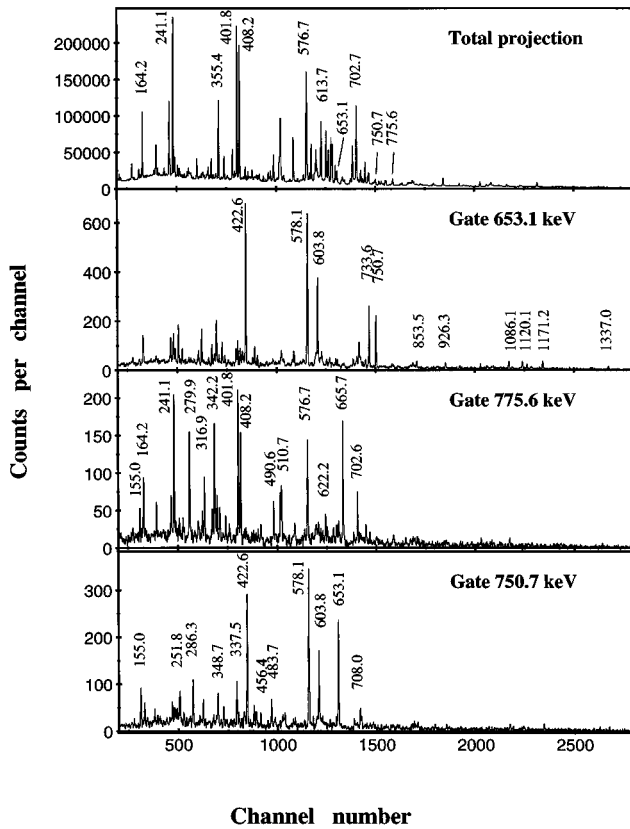


FIG. 1. Examples of γ spectra measured in the $\text{Xe} + ^{15}\text{N}$ reaction at beam energy of 78 MeV. The total projection spectrum is dominated by transitions in ^{147}Pm . The three lower spectra are gated on transitions of ^{145}Pm (indicated in the total projection spectrum).

using the $^{146}\text{Nd}(d, xn)$ reaction at a beam energy of 18 MeV. The target used was a $260 \mu\text{g cm}^{-2}$ foil of isotopically enriched ^{146}Nd deposited on a carbon foil ($38 \mu\text{g cm}^{-2}$). Electron- γ and γ - γ coincidences were measured using the electron-gamma spectrometer operating at the MP-tandem accelerator at Orsay [14] in coincidence with four Compton-suppressed Ge detectors. A total amount of 1.1×10^6 e - γ and 1.3×10^6 γ - γ coincidence events were collected, respectively.

III. DATA ANALYSIS AND RESULTS

A. High-spin data

For the off-line analysis the experimental data were sorted into three-dimensional γ - γ -time and γ - γ -fold histograms. The γ - γ -time cube contained events consisting of two γ -ray energies and a time signal between them. In the γ - γ -fold cube the fold information corresponded to a multiplicity signal measured by the multiplicity filter. Two-dimensional γ - γ histograms with gamma signals gated on detector position were produced and used to determine DCO ratios.

The assignment of γ rays to the ^{145}Pm nucleus was based on a coincidence relation between the 750.7 keV, 775.4 keV, and 653.1 keV transitions reported in the previous in-beam study of ^{145}Pm [5–7]. Spectra gated on these lines, shown in Fig. 1, were used to find relative intensities of γ rays. The

relative intensities of gating transitions were estimated from the total projection of the coincidence data (no single spectra were available). In order to deduce the multipolarity of γ rays DCO ratios were determined (see, e.g., [15]). The analysis of time signals from γ - γ -time spectra did not show any isomer with a lifetime longer than 10 ns, apart from the 794.7 keV level. Therefore apart from the 794.7 keV transition, all other stretched quadrupole transitions in ^{145}Pm , with an energy $E_\gamma < 800$ keV, should have an $E2$ character. This suggestion follows from the fact that no enhanced $M2$ transitions are observed.

B. Low-spin and electron-conversion data

In order to analyze electron-conversion data, coincidence events were sorted into two-dimensional e - γ and γ - γ histograms. Using coincidence data allowed the production of clean electron and γ -ray spectra, gated on a coincident γ line, avoiding problems caused by contamination peaks and a high density of lines. Examples of corresponding gated γ -ray and electron spectra are shown in Fig. 2.

Internal conversion coefficients for γ transitions in ^{145}Pm obtained from the analysis of e - γ and the corresponding γ - γ coincidence data are shown in Fig. 3 against theoretical values [16] for various multiplicities of γ rays in promethium. The coefficients were normalized to reproduce theoretical values of conversion coefficients for the 454 keV and the 590 keV, $E2$ transitions of ^{146}Nd , which are present in the spectra due to Coulomb excitation of target nuclei.

The properties of γ transitions in ^{145}Pm (measured in both reactions used) including energies, relative intensities, the corresponding DCO ratios, and internal conversion coefficients are listed in Table I. In Table I we also show the multiplicities of γ transition deduced from the DCO and internal conversion coefficients values. In the last column the energy of the excited level in ^{145}Pm depopulated by the corresponding γ transition is given.

IV. LEVEL SCHEME OF ^{145}Pm

Most of the previously reported data concerning the excitation scheme of ^{145}Pm [5–7] are confirmed in the present work, while 20 new transitions and 10 new levels are introduced in ^{145}Pm . Below we discuss the construction of the level scheme.

A. Low-spin excitation

The low-spin part of the level scheme of ^{145}Pm is shown in Fig. 4. We confirm most levels previously reported [2–5] except several low-spin levels reported in [5,3], which probably were not populated in our reactions.

To the ground state band we add the 1896.5 keV level deexciting through the 247.0 keV and 489.7 keV transitions. The spin and parity of this level are $I^\pi = \frac{17}{2}^+$, based on the internal conversion coefficient for the 247.0 keV transition. The 442.2 keV decay from the 1649.5 keV level is introduced as well.

The band on top of the $I^\pi = \frac{7}{2}^+$, 61.3 keV level has been updated with the 633.5 and 497.3 keV transitions. Their $E2$ multipolarity, deduced from conversion coefficients and DCO ratios, allowed positive parity assignment for the

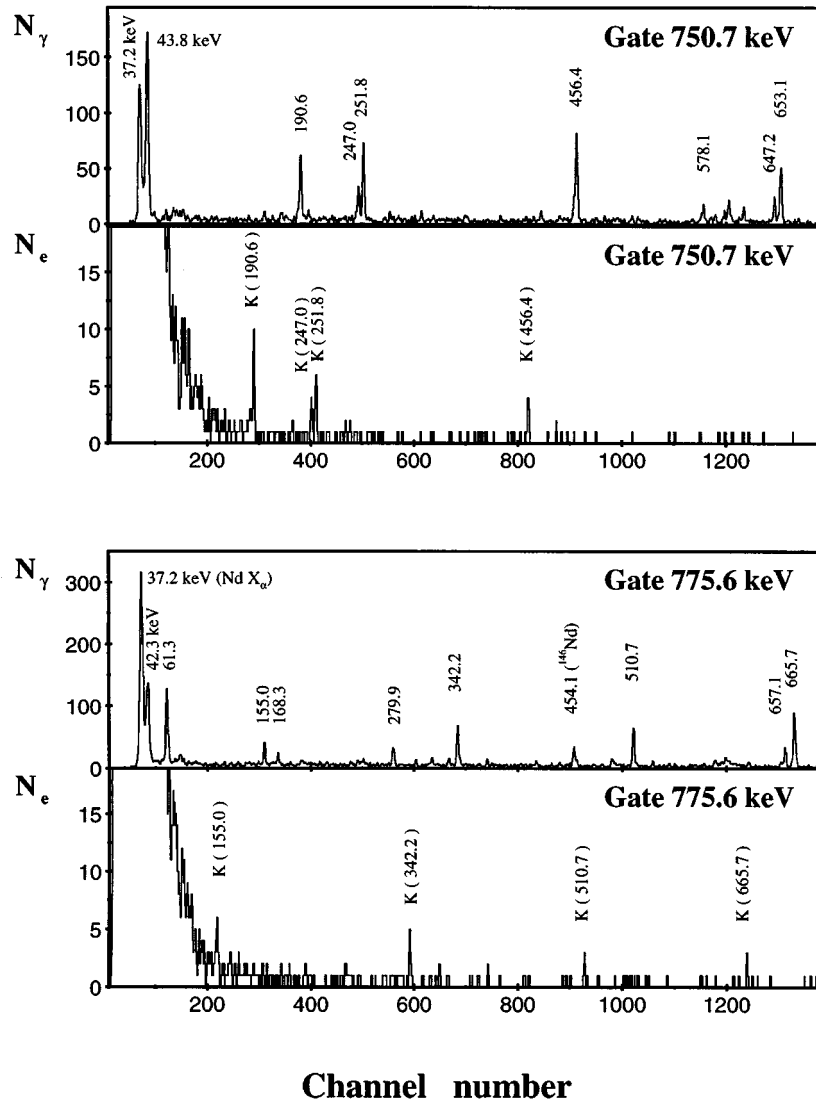


FIG. 2. Examples of gated γ and electron spectra measured in the $^{146}\text{Nd}(d,xn)^{145}\text{Pm}$ reaction at a beam energy of 18 MeV. Energy calibration is 0.5 keV per channel for all four spectra.

1844.8 keV level, reported in Refs. [6,7]. This result is supported by the α_K conversion coefficient for the 342.4 keV transition. The α_K coefficient for the 279.9 keV transition assigns a positive parity to the 2124.7 keV level.

In Ref. [5] the $\frac{7}{2}^-$ level at 1284.0 keV has been reported, decaying via an $E1$, 570.4 keV transition to the $\frac{9}{2}^+$, 713.6 keV level. We observe a level at 1285.0 keV and assign negative parity to it, based on the α_K coefficients for the 570.9 keV transition. For its spin we propose $\frac{7}{2}^-$, rather than $\frac{7}{2}^-$ reported in Ref. [5], because of the likely presence of the 62.0 keV transition from the $\frac{13}{2}^+$, 1347.4 keV state. Though the 62.0 keV transition cannot be resolved from the 61.3 keV one, the coincidence between the 570.9 keV and 155.0 keV transitions suggests its presence. Let us note that if the spin of the 1285.0 keV level was $\frac{7}{2}^-$ as proposed in [5], then one should observe strong $E1$ transition from this level to the 61.3 keV level. Such a transition is not observed in our data. We also add the 1494.0, 1836.7, and 2013.4 keV levels to this part of the scheme. Although they are drawn “in band,” no transitions between them have been observed.

B. 794.7 keV isomer

The 794.7 keV isomeric state has been identified in Ref. [2] with a half-life $T_{1/2} = 18.3(1.9)$ ns and two isomeric transitions were reported, the 734 keV, $M2$ transition and the (unobserved) 44 keV, $E1$ transition. In Ref. [3] the 794 keV, $E3$ isomeric transition has been found in addition. The isomer has been also studied in [5] where a half-life $T_{1/2} = 16.3(1.5)$ ns has been measured. The present work gave $T_{1/2} = 17(2)$ ns and we have identified another decay branch for the isomeric level. The 80.7 keV transition linking the isomer to the 714.0 keV level is clearly seen in our data and there are arguments to show that it is different from the 80.8 keV transitions linking the 750.7 and 670.6 keV levels. Relevant gated spectra are displayed in Fig. 5 and the decay of the isomer is shown in Fig. 6.

The spectrum in Fig. 5(a) is a sum of spectra gated on the 456.4 keV and 647.2 keV lines (see Fig. 4). From this spectrum one can estimate gamma branching between the 80.8 keV and 750.7 keV transitions depopulating the 750.7 keV level. Its value is 0.02(1), in agreement with previous mea-

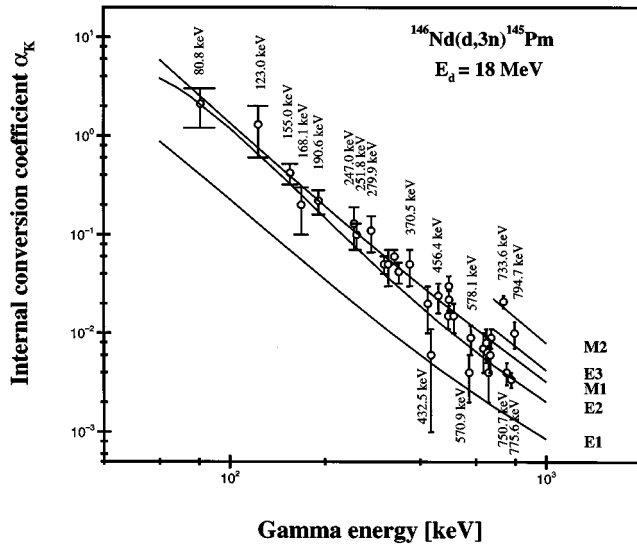


FIG. 3. Internal conversion coefficients α_K obtained from the electron- γ coincidences measured using the $^{146}\text{Nd}(d,3n)^{145}\text{Pm}$ reaction at a beam energy of 18 MeV. Solid curves represent theoretical α_K conversion coefficients in promethium taken from Ref. [16].

measurements [17]. Considering the intensities of the 750.7 keV, 670.0 keV, and 608.6 keV lines, the total intensity of the 80.8 keV transition can be estimated as 0.12(2) of the intensity of the 750.7 keV line. This result is consistent with previous studies and provides an estimate of the total conversion coefficient for the 80.8 keV transition ($\alpha_{\text{tot}} \approx 5$) consistent with its $M1/E2$ character inferred from the decay scheme and confirmed by the α_K coefficient obtained from our e - γ measurement. On the other hand, the gamma branching between the 81 keV and 750.7 keV lines in the spectrum gated on the 653 keV line [Fig. 5(b)] has a value of 0.15(3), indicating that there is another component in the 81 keV line, apart from the known 80.8 keV transition. Figure 5(b) shows that the 653 keV transition is self-gating. An 80.7 keV link between the 794.7 keV and the 714.0 keV levels could explain this fact. It should be mentioned that in Ref. [5] the 652.4 keV transition from the 1365.9 keV level to the 714.0 keV level has been introduced which could account for the self-gating. We can not confirm the existence of the 1365.9 keV level because the 529.4 keV transition from this level, reported in [5], is not seen in our data. Consequently, we assume that the self-gating effect is due to the coincidence between the 653.1 keV and 652.7 keV γ rays. This is confirmed further by gating on the 81 keV line. Figure 5(c), shows the gated spectrum. Again, data suggest the proposed link because the intensity of the 653 keV line is larger than the intensity of the 670.0 keV line. The 608.6 keV line is hardly visible in the spectrum and can not account for this difference.

From spectra gated on the 307.5 keV and 787.7 keV lines we could estimate total intensity of the 80.7 keV transition, assuming that it is equal to the γ intensity of the 652.7 keV line seen in this spectrum. The total intensity obtained in this way is 12(3)% of the intensity of the 733.6 keV line. Taking this total intensity and the γ intensity of the 80.7 keV line from this spectrum we could estimate total conversion coef-

ficient for the 80.7 keV transition to be 0.5(3), which is consistent with an $E1$ character expected for this transition.

C. High-spin excitation

High-spin states in ^{145}Pm have been studied previously in the $^{19}\text{F} + ^{130}\text{Te}$ reaction up to spin $\frac{33}{2}$ and excitation energy of 4.7 MeV [6,7]. In the present work we have extended the level to an excitation energy of 7.2 MeV and still higher spins. The high-spin part of the level scheme of ^{145}Pm resulting from the present work is shown in Fig. 6.

Transitions and levels have been placed according to coincidence relations between γ rays. In most cases it was possible to deduce spins from measured DCO coefficients. There is, however, no direct measurement providing parities for high-spin levels, except conversion electron coefficients for the 653.1, 578.1, and 422.6 keV transitions. In this situation we suggested parity assignments based on measured DCO ratios and observed branching ratios. Our assignments mostly agree with spin and parity assignments of Refs. [6,7]. There are however, a few differences. The spin of the 4223.5 keV level is most likely $\frac{29}{2}$ rather than $\frac{31}{2}$ proposed earlier because of the $\Delta I = 1$ character of the 1171.2 keV transition. The DCO for the 1337.0 keV transition suggests spin $\frac{29}{2}$ for the 4389.7 keV level instead of $\frac{31}{2}$ proposed earlier. Consequently the most likely spins of the spin 3665.1 keV and the 4086.2 keV levels are $\frac{25}{2}$ and $\frac{27}{2}$, respectively.

V. INTERPRETATION

The nucleus ^{145}Pm has three proton holes and two neutrons outside the double closed shell nucleus ^{146}Gd . Consequently, one expects weak deformation and multiparticle excitations dominating the level scheme, as observed in the $N = 84$ isotones ^{147}Eu [18,19] and ^{149}Tb [1,8]. At low energies, proton excitations corresponding to the $g_{7/2}, d_{5/2}$, and $h_{11/2}$ proton orbitals were reported previously [2–5]. High-spin, multiparticle excitations are expected to be due to neutrons in $f_{7/2}, h_{9/2}$ or $i_{13/2}$ orbitals, coupled to the $h_{11/2}$ proton excitation. Such configurations are commonly observed in the $N = 84$ isotones ^{144}Nd , ^{146}Sm , and ^{149}Tb . At still higher energies, where available neutron configurations are exhausted, one may expect excitations due to breaking of the proton core and promoting another proton to the $h_{11/2}$ orbital, similarly as observed in ^{149}Tb [1,8]. Angular momentum can be generated also by aligning pairs of $d_{5/2}$ or $g_{7/2}$ proton holes. This has been observed in ^{149}Tb [1,8] but only at high spins. In contrast to these observations the authors of Refs. [6,7] suggest that in ^{145}Pm aligning $d_{5/2}$ or $g_{7/2}$ proton-hole pairs takes place at quite low spin and that the breaking of the proton core and the promoting two protons to the $h_{11/2}$ orbital happen already at spin $I = 8$ in ^{144}Nd and at spin $I = 27/2$ in ^{145}Pm .

Besides the multiparticle excitations, collective excitations of a vibrational character coupled to those multiparticle configurations are expected in ^{145}Pm . A very characteristic type of collective excitations in this region is octupole vibrations (see, e.g., Ref. [20]). Octupole phonon excitations are expected in ^{145}Pm , because of pronounced octupole vibrations observed in the core nuclei ^{144}Nd and ^{146}Sm [21–24]. Quadrupole vibrations should also be present but they may

TABLE I. Energies, intensities, DCO ratios, and α_K internal conversion coefficients for transitions in ^{145}Pm measured in the present work. Errors of γ -ray energies are $\Delta E=0.1$ keV for strong transitions ($I_\gamma > 30$), $\Delta E=0.2$ keV for transitions with $30 > I_\gamma > 10$, and $\Delta E=0.3$ keV for weak transitions ($I_\gamma < 10$).

E_γ (keV)	I_γ ^a	I_γ ^b	R_{DCO}	α_K ^c	Multipolarity ^d	E_{ex} (keV)
44						794.7
61.3		40(4)				61.3
62.0						1347.6
80.7		2(1)		0.5(3) ^e	<i>E1</i>	794.7
80.8		2(1)		2.1(9)	<i>M1 + E2</i>	750.7
123.0		3.3(9)		1.3(7)	<i>M1 + E2</i>	836.6
138.7	5(1)		2.2(7)			4362.4
155.0		9(1)		0.42(10)	<i>M1 + E2</i>	1502.6
163.3		1.0(5)				824.1
164.5	7(2)		2.0(5)			5891.6
168.1		1.1(3)		0.2(1)	<i>M1 + E2</i>	660.8
168.6		4(1)				2013.4
190.6		14(2)		0.22(6)	<i>M1 + E2</i>	1397.8
196.3	6(1)					2811.5
233.8	9(1)					4935.0
239.0	6(2)					6130.6
244.6	5.5(8)		1.5(3)			5727.1
247.0		8(1)		0.13(6)	<i>M1 + E2</i>	1896.5
251.8		18(2)		0.10(3)	<i>M1 + E2</i>	1649.5
253.4	13.2(8)		1.3(2)			4013.8
263.3	5.8(7)					3760.3
279.9		12(2)	1.3(2)	0.11(4)	<i>M1 + E2</i>	2124.7
283.1		3(1)				1385.3
303.5	4(1)					4389.7
307.5	4(2)	5(2)		0.05(1)	<i>M1 + E2</i>	1102.2
311.7	12(2)		1.9(5)			4701.4
316.9	7(1)	5(1)	1.6(3)	0.05(2)	<i>M1 + E2</i>	2441.3
331.4		3.2(5)		0.06(1)	<i>E2</i>	824.1
334.1		10(2)				1836.7
337.2	11(2)					3497.0
342.2		27(4)	1.5(3)	0.04(1)	<i>M1 + E2</i>	1844.8
348.2	5(2)					3160.0
348.8	15(2)		1.45(18) ^f			4362.4
362.9	8.3(7)		1.0(2)			2811.5
369.9	9(1)					2811.5
370.5		6(2)		0.05(2)	<i>M1 + E2</i>	1207.1
388.0						1102.2
397.8	7(1)		0.8(3)			4760.2
403.5	1.0(5)					6130.6
409.0	2.0(5)					5891.6
415.4	4.5(8)	3(1)				2441.3
421.0	6(1)					4086.2
422.6	72(3)	6(1)		0.02(1)	<i>E2</i>	2448.5
432.5		3(1)		0.006(5)	<i>E1</i>	1102.2
442.2		4(1)				1649.5
444.6	8.2(8)		0.85(15)			3497.0
456.4		35(3)		0.024(8)	<i>M1 + E2</i>	1207.1
490.6	7(1)	5(1)	1.4(4)	0.015(4)	<i>M1 + E2</i>	2615.3
492.7		23(2)		0.030(8)	<i>M1 + E2</i>	492.7
493.2		8(2)		0.022(5)	<i>M1 + E2</i>	1207.1
497.3		5(2)		0.05(2)	<i>E2</i>	1844.8

TABLE I. (Continued).

E_γ (keV)	I_γ^a	I_γ^b	R_{DCO}	α_K^c	Multipolarity ^d	E_{ex} (keV)
498.7		1.0(5)				1896.5
510.7		23(3)		0.015(5)	$M1 + E2$	1347.6
516.9	4.5(7)					4013.8
537.1		2(1)				1207.1
539.0	2(1)					4389.7
544.6	4(2)					3160.0
545.5						4935.0
570.9		21(3)		0.004(2)	$E1$	1285.0
578.1	95(5)	23(3)		0.009(3)	$E2$	2025.8
599.5						660.8
600.5	2.9(5)					3760.3
603.8	45(2)					3052.3
608.6		3(1)				670.0
613.0	5(1)					3665.1
615.3	3(1)					4701.4
622.2		9(1)				2124.7
633.5		13(3)		0.007(3)	$E2$	1347.6
647.2		10(2)				1397.8
652.7	18(2)	35(5)				714.0
653.1	100(5)	50(5)			$E2^g$	1447.8
657.1		10(2)				1494.0
660.7						660.8
665.7	21(2)	33(4)	0.9(3)	0.006(2)	$E2$	1502.6
670.0	7.1(7)	28(2)		0.009(2)	$M1 + E2$	670.0
708.0	17(1)		2.1(3)			3760.3
711.3	1.5(5)					4935.0
711.6	7.5(5)		1.8(4)			3160.0
718.3	5(1)					3160.0
724.4	4(1)					4389.7
733.6	51(3)	35(4)		0.021(3)	$M2$	794.7
750.7	42(3)	99(5)		0.004(1)	$E2^g$	750.7
762.5		3(1)				824.1
775.6		100(5)		0.004(1)	$E2^g$	836.6
787.8	3(1)	8(2)		0.011(3)		1582.5
794.7	2.2(5)	5.5(5)		0.010(3)	$E3$	794.7
806.8	2.3(8)					5030.3
853.8	5.3(7)		1.5(4)			3665.1
926.2	6.0(9)		2.0(6)			4086.2
962.0	3.1(8)					6853.6
1034.0	0.8(4)		≈ 1			4086.2
1040.7	9(3)	8(2)				1102.2
1086.1	7.4(9)		1.6(3)			7216.7
1120.1	7.8(9)		0.9(2)			5482.5
1131.4	3.9(8)		1.0(3)			5891.6
1171.2	10(1)		1.9(2)			3851.0
1337.0	4.1(7)		1.9(5)			4389.7
1402.5	1.0(5)		≤ 1			3851.0

^aRelative intensities measured in the $^{134}\text{Xe}(^{15}\text{N},4n)^{145}\text{Pm}$ reaction at beam energy of 78 MeV where $I_\gamma(653.1 \text{ keV}) = 100$.

^bRelative intensities measured in the $^{146}\text{Nd}(d,3n)^{145}\text{Pm}$ reaction at beam energy of 18 MeV where $I_\gamma(775.6 \text{ keV}) = 100$.

^c α_K conversion coefficients obtained from $e-\gamma$ coincidence data, unless indicated otherwise.

^dAdopted.

^eTotal conversion coefficient obtained from intensity balance.

^fReference $\Delta I=2$ transition.

^gDCO ratio for 348.8 keV + 348.2 keV doublet.

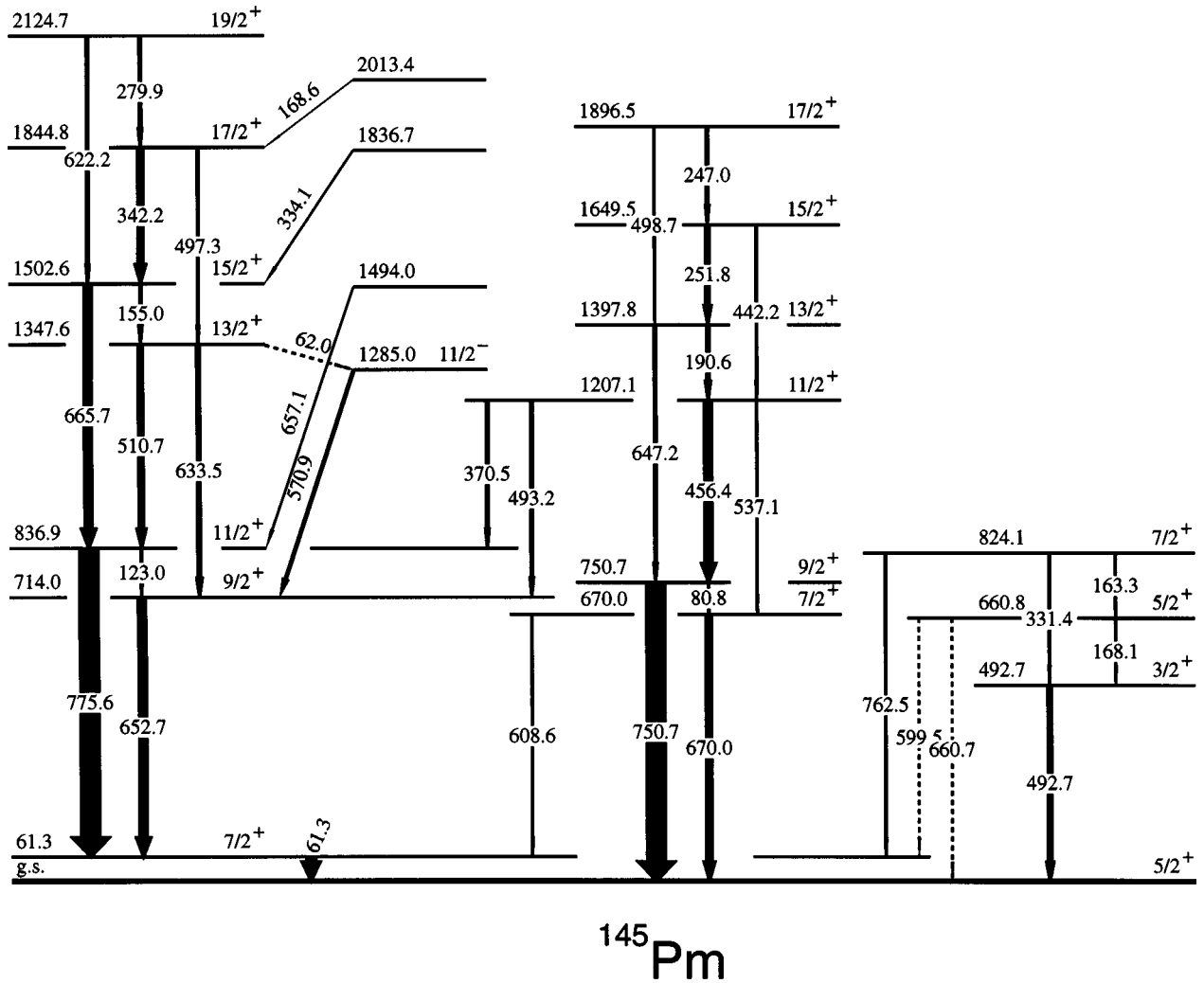


FIG. 4. Low-spin excitations of ^{145}Pm observed in the present work (see Fig. 6 for feeding of the 2124.7 keV level). Widths of arrows are proportional to the I_γ in the $^{146}\text{Nd}+d$ reaction.

be mixed with bandlike structures arising from decoupling of pairs of particles such as $(f_{7/2}^2)_{0^+,2^+,4^+,6^+}$ or holes such as $(d_{5/2}^-2)_{0^+,2^+,4^+}$, which are observed in the neighboring nuclei. Below we discuss in more detail various excitations in ^{145}Pm observed in the present work.

A. Excitations on top of the $d_{5/2}$ and $g_{7/2}$ proton levels

The ground state of ^{145}Pm and the excited levels at 61.3 keV have been established in studies of β decay of ^{145}Sm [25] and confirmed by a number of other works (see Ref. [17] and references therein). These states were interpreted as $d_{5/2}$ and $g_{7/2}$ single-particle proton levels, respectively [2,4].

Bands of $E2$ and $M1 + E2$ transitions have been found on top of the ground state and the 61.3 keV level [5], which have been extended in the present work up to spin $I = \frac{17}{2}^+$ and $I = \frac{19}{2}^+$, respectively. These bands have been described in Ref. [5] in frame of the cluster-vibration model as due to coupling between a quadrupole phonon and a cluster of three proton holes in $d_{5/2}$ and $g_{7/2}$ orbitals. Since the calculations presented in Ref. [5] are limited to levels with spin $I \leq \frac{15}{2}^+$, levels with higher spins cannot be compared with the predic-

tions of the cluster-vibration model. However, one may note the following.

(i) The cluster-vibration model reproduces the experimental data with a moderate accuracy. In particular it predicts stronger than observed links between the two bands while the new experimental evidence stresses the fact that the two bands are separate.

(ii) Calculations presented in Ref. [5] do not take into account the presence of a pair of neutrons in ^{145}Pm .

(iii) In the present work both bands are observed over a spin range of $6\hbar$ only and it seems that this truncation is not due to experimental limitations.

Considering these observations another interpretation is plausible, namely, that the two bands are due to a recoupling of the pair of neutrons in the $f_{7/2}$ orbital, a phenomenon which is commonly observed in the neighboring nuclei. Such an interpretation has been already proposed in Refs. [6,7] but it has to be discussed again because of an improper assignment of levels to bands done in Refs. [6,7]. The $\frac{13}{2}^+$, 1347.6 keV and $\frac{17}{2}^+$, 1844.8 keV levels were assigned to the band on top of the ground state. This produces a situation where both bands contain three levels each and can be therefore

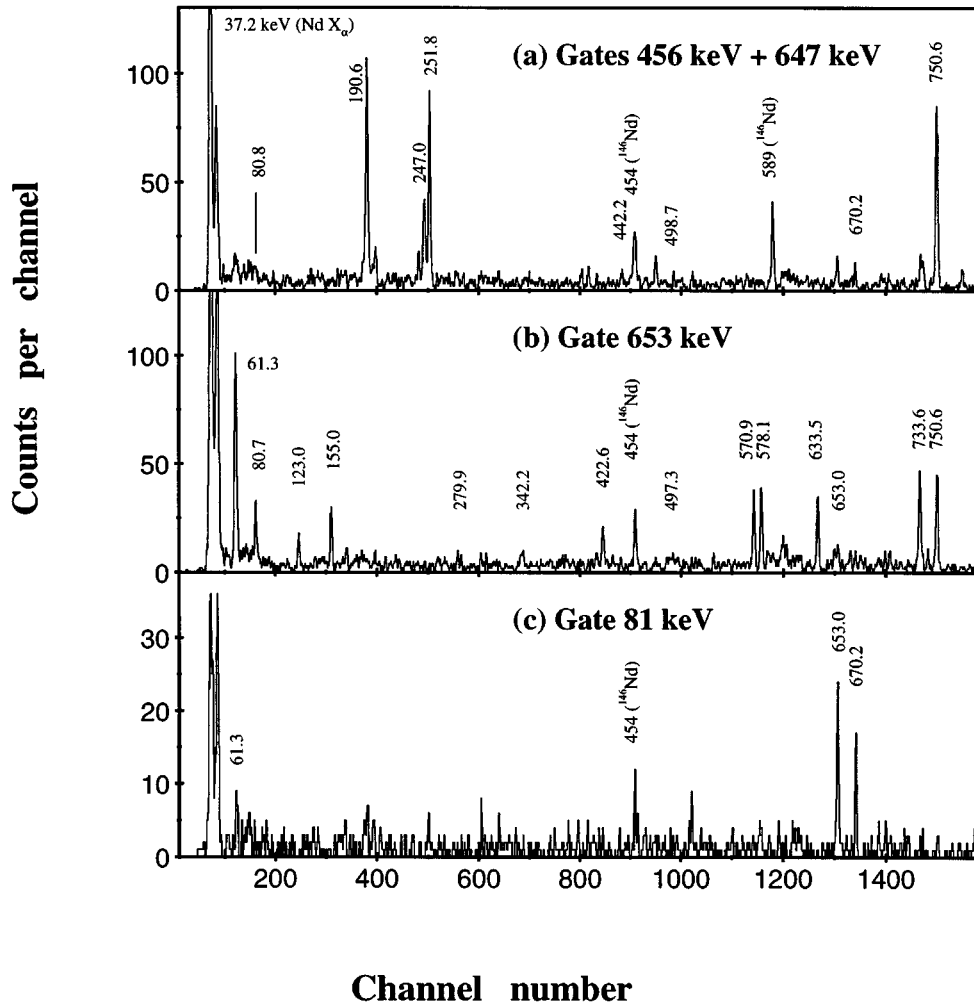


FIG. 5. Spectra illustrating the presence of the 80.7 keV transition.

accounted for by coupling the $(f_{7/2}^2)_{0^+,2^+,4^+,6^+}$ multiplet to the $d_{5/2}$ or $g_{7/2}$ proton orbitals. However, the present data show that each of the two bands contain seven levels. The levels in the band decay readily to each other but there is little communication between the two bands. Coupling of the $(f_{7/2}^2)_{0^+,2^+,4^+,6^+}$ sequence to the $d_{5/2}$ or $g_{7/2}$ proton orbitals can reproduce all seven levels in each band if one notices that the “unfavored” members of the bands may result from a noncomplete alignment of the $(f_{7/2}^2)_{0^+,2^+,4^+,6^+}$ multiplet relative to the $d_{5/2}$ or $g_{7/2}$ proton-hole states.

B. Excitations on top of the $h_{11/2}$ proton level

The close similarity of high-spin excitations on top of the $h_{11/2}$ proton level in ^{145}Pm to analogous excitations in ^{149}Tb suggests a similar interpretation to that proposed in [1,8] for ^{149}Tb . In ^{149}Tb three types of excitations have been identified on top of the $h_{11/2}$ proton level: (i) a group of negative-parity levels right on top of the isomeric level, which were described as the $f_{7/2}, h_{9/2}$ or $i_{13/2}$ neutron configurations coupled to the $h_{11/2}$ proton level, (ii) a group of positive parity levels coupled to the neutron configurations mentioned in (i), and (iii) a group of high-spin states which were interpreted as due to breaking proton core and promoting another proton to the $h_{11/2}$ orbital.

All three types of excitations are observed in ^{145}Pm and two other structures have been identified in the present work. Below we discuss these excitation in more detail.

1. $\pi h_{11/2} \otimes \nu^2$ configurations

At low excitation energy in ^{145}Pm two valence neutrons in the $f_{7/2}$ orbital form a characteristic $(f_{7/2}^2)_{0^+,2^+,4^+,6^+}$ multiplet, coupled to the $h_{11/2}$ proton level. Levels at 794.7, 1447.8, 20025.9, and 2448.5 keV result from this coupling, as already noticed in [6]. The maximum-aligned member of this multiplet in ^{145}Pm is compared in Fig. 7 with analogous excitations in ^{147}Eu and ^{149}Tb isotones and with the results of semiempirical calculations for the $[\pi h_{11/2} \nu(f_{7/2}^2)_{6^+}]_{23/2^-}$ configuration in ^{145}Pm , similar to those performed in Ref. [1].

At higher excitation energy one of the neutrons is promoted to the $h_{9/2}$ orbital and the $[\pi h_{11/2} \otimes \nu(f_{7/2} h_{9/2})_{8^+}]_{27/2^-}$ configuration is produced, which accounts for the 3052.3 keV level in ^{145}Pm . In Fig. 7 the discussed level in ^{145}Pm is compared to analogous excitations in ^{147}Eu and ^{149}Tb isotones. The good reproduction of the experimental data by the calculations and systematic agreement with excitation energies of analogous levels in the neighboring nuclei supports the proposed interpretation for

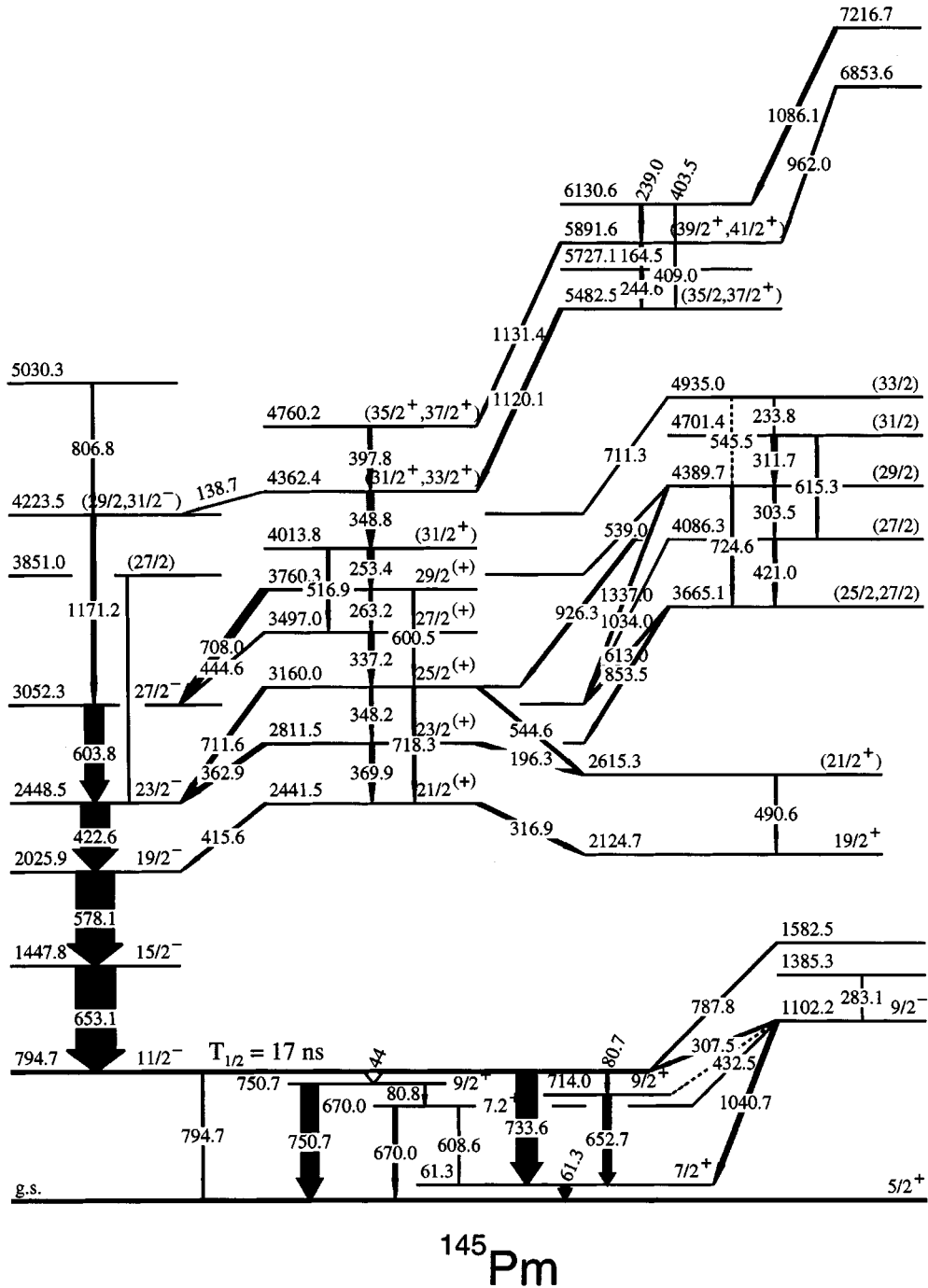


FIG. 6. High-spin excitations of ^{145}Pm as observed in the present work. See Fig. 4 for decay of the 2124.7 keV level and other feeding of of the 670.0, 714.0, and 750.7 keV levels. Widths of arrows are proportional to the I_γ in the $^{134}\text{Xe} + ^{15}\text{N}$ reaction.

the 2448.5 keV and 3052.3 keV levels.

It should be mentioned that the 3052.3 keV level was interpreted differently in two previous works. In Ref. [7] a coupling of the 8_1^+ excitation in ^{144}Nd to the $h_{11/2}$ proton level was proposed as the explanation, where the 8_1^+ in ^{144}Nd was interpreted as a $h_{11/2}^2$ structure. Three protons in the $h_{11/2}$ orbital can indeed couple to the maximum spin of $I^\pi = \frac{27}{2}^-$. However, a rough estimate of excitation energy for such a $[h_{11/2}^3]_{27/2^-}$ configuration (3 times the $h_{11/2}$ proton excitation + pairing gap) shows that such an excitation is expected well above the experimentally observed $27/2^-$, 3052.3 keV level. The same 3052.3 keV level was inter-

preted in Ref. [6] as due to aligning of proton holes in the $d_{5/2}$ and/or $g_{7/2}$ orbitals. Although this interpretation can not be excluded, let us note that calculations assuming neutron involvement reproduce essentially better the level energy [3169 keV for the $\nu(f_{7/2}h_{9/2})$ configuration as compared to 3338 keV for proton holes configuration [6]]. It is possible that both $(f_{7/2}h_{9/2})$ neutron and $d_{5/2}$ or $g_{7/2}$ proton-hole configurations contribute to the $27/2^-$, 3052.3 keV excitation.

Above the $[\pi h_{11/2}\nu(f_{7/2}h_{9/2})_8^+]_{27/2^-}$ configuration more angular momentum can be generated either by exciting one of valence neutrons to the $i_{13/2}$ orbital or by aligning proton holes. The 4223.5 keV level was interpreted [6] as

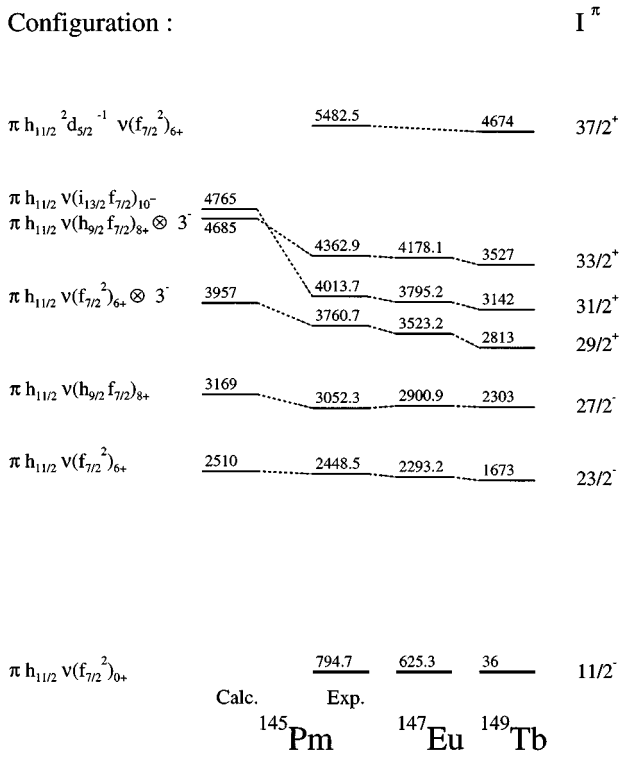


FIG. 7. Systematics of multiparticle excitations in the odd- $Z, N=86$ lanthanides. Data for ^{149}Tb and ^{147}Eu are taken from Refs. [1,18,19]. Note that levels are labeled with their energies relative to the ground state but are drawn relative to the $11/2^-$ excitation. Calculated levels are drawn relative to the 794 keV level.

due to aligning proton holes and assigned the $[\pi h_{1/2}(d_{5/2}^{-2})_{2+} \nu(f_{7/2})_{6+}]_{31/2^-}$ configuration. Considering the new interpretation proposed above for the 3052.3 keV level, one may note that if the spin of the 4223.5 keV level is $\frac{31}{2}^-$ as proposed in [6], the $[\pi h_{1/2} \nu(h_{9/2} f_{7/2})]_{31/2^-} \otimes (d_{5/2}^{-2})_{2+,4+}$ configuration could account for the 4223.5 keV and 5030.3 keV levels (assuming spin $I^\pi = \frac{35}{2}^-$ for the latter one). However, the present data suggest for the 4223.5 keV level spin $I = \frac{29}{2}$, leaving open the question about its nature. It has been argued that the 3142 keV level in ^{149}Tb has a $[\pi h_{1/2} \nu(f_{7/2} i_{13/2})]_{31/2^+}$ configuration [1]. In Fig. 7 analogous levels in ^{145}Pm and ^{147}Eu are shown. This systematics suggests similar interpretation for the level at 4013.8 keV in ^{145}Pm . However, semiempirical calculations for this configuration in ^{145}Pm predict excitation energy of 4765 keV, well above the experimental value, leaving open the question about the interpretation of this level. Let us note that configurations containing proton holes are excluded because aligning a pair of proton and holes on top of the $\pi h_{1/2} \nu(f_{7/2})_{6+}$ level produces states of negative parity while the maximum aligned coupling of $[\pi(d_{5/2}^{-1} g_{7/2}^{-2})_{17/2^+} (f_{7/2})_{6+}]_{29/2^+}$ does not produce enough angular momentum to explain the $\frac{31}{2}^+$, 4013.8 keV level.

When the other neutron is excited to the $h_{9/2}$ orbital a maximum aligned configuration $[\pi h_{1/2} \nu(h_{9/2} i_{13/2})]_{33/2^+}$ is formed. A possible candidate for this configuration in ^{145}Pm is the 4362.4 keV level. But as will be discussed below this level could be due to octupole excitation.

2. Possible $\pi h_{1/2} \nu^2 \otimes (\pi^{-2})_j$ configurations

The levels at 3665.1, 4086.2, 4389.7, 4701.4, and 4935.0 keV have no counterparts in ^{149}Tb . This suggests that they may be due to proton-hole excitations of a $(\pi h_{1/2} \nu^2) \otimes (\pi^{-2})_j$ type, which are absent in ^{149}Tb . More exact statements are, however, not possible at present since we could not establish the parities of these levels. If the above proposition is correct, the discussed levels should have negative parity. On the other hand, if the parity of the 4701.4 keV level is positive, it could be well described by the $[\pi h_{1/2} \nu(f_{7/2} i_{13/2})]_{31/2^+}$ configuration, mentioned above (see Fig. 7).

3. Possible $\pi h_{1/2}^2 \nu^2$ configurations

Promotion of another proton to the $h_{1/2}$ orbital allows us to generate still more angular momentum. The $(\frac{35}{2}, \frac{37}{2}^+)$, 5482.5 keV level is a candidate for the $[\pi(h_{1/2}^2 d_{5/2}^{-1}) \nu(f_{7/2})_{6+}]_{37/2^+}$ configuration. High-energy decay from this level supports the idea of proton promotion. An analogous level is observed in ^{149}Tb (see Fig. 7). On top of this level we do observe a short cascade. A similar cascade in ^{149}Tb has been interpreted as due to the recoupling of a pair of proton holes in the $[\pi(h_{1/2}^2 d_{5/2}^{-1}) \nu(f_{7/2})_{6+}] \otimes (\pi^{-2})_j$ configuration [1].

At still higher excitation energies there are the 6853.6 keV and 7216.7 keV levels decaying by high-energy transitions. This suggests further particle promotion. It is possible that, in addition to the proton promotion discussed above, one of a neutrons is promoted from the $f_{7/2}$ to the $i_{13/2}$ orbital as suggested for an analogous states in ^{149}Tb by the deformed independent particle model calculations performed in [8].

C. Octupole excitations

Octupole phonon vibrations observed in the core nucleus ^{144}Nd [21,23,24] are expected to form in ^{145}Pm excitations resulting from coupling of this phonon to multiparticle configurations. Analogous octupole phonon excitations coupled to $\pi h_{1/2} \nu^2$ configurations were recently found in ^{149}Eu [26]. An interesting observation in this case is that besides the 3^- octupole excitations one observes also the 2^- coupling. This results from Pauli blocking of an octupole phonon to which the $\pi h_{1/2} d_{5/2}$ pair contributes. As a result one observes a band of positive parity levels, spaced by $\Delta I=1$ in spin, which are interconnected by $M1$ and $E2$ transitions. These band decay by pronounced $E1$ transition to the yrast band on top of the $\pi h_{1/2}$ state [26].

The 2441.5, 2811.5, 3160.0, 3497.0, 3760.3, 4013.8, and 4362.4 keV levels in ^{145}Pm form such a band and are therefore likely candidates for octupole phonon excitations. Analogous excitations, interpreted as an octupole phonon coupled to the $\pi h_{1/2} \nu^2$ configuration, were observed in ^{149}Tb [1]. Two of these levels, observed systematically in ^{149}Tb , ^{147}Eu , and ^{145}Pm , are shown in Fig. 7 and are interpreted as $[\pi h_{1/2} \nu(f_{7/2})]_{23/2^-} \otimes 3^-$ and $[\pi h_{1/2} \nu(f_{7/2} h_{9/2})]_{27/2^-} \otimes 3^-$ configurations, respectively, which is supported by the result of semiempirical calculations for levels in ^{145}Pm . The proposed octupole excitation coupled to the $[\pi h_{1/2} \nu(f_{7/2} h_{9/2})]_{27/2^-}$ configuration satisfac-

torily describes the 4362.4 keV level but the contribution from the $[\pi h_{11/2} \nu(h_{9/2} i_{13/2})]_{33/2^+}$ configuration, discussed in the previous section, cannot be excluded.

It should be mentioned that some of the levels discussed above were described in Ref. [6] as members of the $[\nu(f_{7/2}^2) \otimes \pi^{-3}]_j$ multiplet. Indeed, semiempirical calculations predict an excitation energy of 3730 keV for the $[\nu(f_{7/2}^2)_{6^+} \otimes \pi(g_{7/2}^{-2} d_{5/2}^{-1})]_{29/2^+}$ configuration, close to the $I^\pi = \frac{29}{2}^+$, 3760.3 keV level. Therefore, although strong $E1$ decays to the $\pi h_{11/2} \nu^2$ band suggest octupole phonon excitations, the contribution from $\nu^2 \pi^{-3}$ cannot be excluded, especially for lower band members, which decay also to the 2124.7 keV and 2615.3 keV levels, most likely of the $\nu^2 \pi^{-3}$ nature.

In ^{145}Pm we have identified another candidate for an octupole excitation, which does not have a counterpart in the known level scheme of ^{149}Tb , possibly because in ^{149}Tb this level is too nonyrast to be observed there. The 1285.0 keV level in ^{145}Pm (see Fig. 4), which has been assigned spin $I^\pi = \frac{11}{2}^-$ is an analog to the 970.0 keV level in ^{147}Pm , interpreted as an octupole excitation coupled to the ground state [11]. On top of the 970.0 keV level in ^{147}Pm a regular band is observed, interpreted as a signature of strong octupole correlations. In ^{145}Pm we observe four possible members of

such a band, which, however, do not decay into each other (possibly because of the unfavored branchings). It is likely that octupole correlations in ^{145}Pm are weaker and do not produce a parity-doublet structure such as observed in ^{147}Pm .

VI. CONCLUSIONS

We have studied medium-to-high-spin excitations in ^{145}Pm using the $^{134}\text{Xe}(^{15}\text{N}, 4n)$ compound nucleus reaction. Several new excited levels were introduced in the level scheme of ^{145}Pm , which allow a more consistent interpretation of this nucleus. Levels in ^{145}Pm are interpreted as multiparticle excitations of the valence particles and holes as well as vibrational collective excitations coupled to them. Octupole excitations observed in ^{145}Pm are due to octupole phonon coupled to multiparticle configurations. This suggests that octupole correlations in ^{145}Pm are weaker than those observed in ^{147}Pm , where a parity-doublet structure has been observed. The present work shows that in ^{145}Pm there are excitations due to two valence neutrons observed systematically in the ^{147}Eu and ^{149}Tb isotones, which have not been considered in previous studies of ^{145}Pm .

-
- [1] M. Lach, P. Kleinheinz, M. Piiparinen, M. Ogawa, S. Lunardi, M.C. Bosca, J. Styczen, and J. Blomquist, *Z. Phys. A* **341**, 25 (1991).
- [2] T. Shibata, Y. Nagai, M. Fujiwara, and H. Ejiri, *Nucl. Phys.* **A257**, 303 (1976).
- [3] Y. Nagai, T. Shibata, S. Nakayama, and H. Ejiri, *Nucl. Phys.* **A282**, 29 (1977).
- [4] O. Straume, G. Løvnhøiden, and D.G. Burke, *Z. Phys. A* **295**, 259 (1980).
- [5] M. Kortelahti, M. Piiparinen, A. Pakkanen, T. Komppa, R. Komu, S. Brant, L.J. Udovičič, and V. Paar, *Nucl. Phys.* **A342**, 421 (1980).
- [6] T. Glasmacher, D.D. Caussyn, P.D. Cottle, T.D. Johnson, K.W. Kemper, and P.C. Womble, *Phys. Rev. C* **45**, 1619 (1992).
- [7] T. Glasmacher, D.D. Caussyn, P.D. Cottle, J.W. Holcomb, T.D. Johnson, K.W. Kemper, M.A. Kennedy, and P.C. Womble, *Phys. Rev. C* **47**, 2586 (1993).
- [8] Z. Méliani, J.S. Dionisio, C. Schück, Ch. Vieu, F.A. Beck, T. Byrski, D. Curien, G. Duchêne, J.C. Merdinger, P. Fallon, J.W. Roberts, and J.F. Sharpey-Schafer, *Nucl. Phys.* **A575**, 221 (1994).
- [9] W. Urban, J.C. Bacelar, W. Gast, G. Hebbinghaus, A. Krämer-Flecken, R.M. Lieder, T. Morek, and T. Rząca-Urban, *Phys. Lett. B* **247**, 238 (1990).
- [10] W.J. Vermeer, M.K. Khan, A.S. Mowbray, J.B. Fitzgerald, J.A. Cizewski, B.J. Varley, J.L. Durell, and W.R. Phillips, *Phys. Rev. C* **42**, R1183 (1990).
- [11] W. Urban, J.L. Durell, W.R. Phillips, B.J. Varley, Ch.P. Hess, M.A. Jones, C.J. Pearson, W.J. Vermeer, Ch. Vieu, J.S. Dionisio, M. Pautrat, and J.C. Bacelar, *Nucl. Phys.* **A587**, 541 (1995).
- [12] T. Rząca-Urban, W. Urban, J.L. Durell, W.R. Phillips, B.J. Varley, Ch.P. Hess, C.J. Pearson, W.J. Vermeer, Ch. Vieu, J.S. Dionisio, M. Pautrat, and J.C. Bacelar, *Nucl. Phys.* **A588**, 767 (1995).
- [13] W. Urban, J.C. Bacelar, O. Dermois, J.R. Jongman, and H. Postma, KVI Annual Report 1989, p. 144; W. Urban, B.J. Varley, and R. King, The University of Manchester, report nuclear physics 1992-1993, p. 93; and (unpublished).
- [14] J.S. Dionisio, C. Vieu, J.M. Lagrange, M. Pautrat, J. Vanhorenbeeck, and A. Passoja, *Nucl. Instrum. Methods A* **282**, 10 (1989).
- [15] A. Krämer-Flecken, T. Morek, R.M. Lieder, W. Gast, G. Hebbinghaus, H.M. Jäger, and W. Urban, *Nucl. Instrum. Methods* **275**, 333 (1989).
- [16] F. Rösel, H.M. Fries, K. Alder, and H.C. Paul, *Nucl. Data Nucl. Data Tables* **21**, 1 (1978).
- [17] L.K. Peker, *Nucl. Data Sheets* **68**, 997 (1993).
- [18] J.G. Fleissner, E.G. Funk, F.P. Venezia, and J.W. Mihelich, *Phys. Rev. C* **16**, 227 (1977).
- [19] G. Lo Bianco, N. Molho, A. Moroni, A. Bracco, and N. Blasi, *J. Phys. G* **7**, 219 (1981).
- [20] P.D. Cottle and D.A. Bromley, *Phys. Lett. B* **182**, 129 (1986); *Phys. Rev. C* **35**, 1891 (1987).
- [21] P.D. Cottle, S.M. Aziz, J.D. Fox, K.W. Kemper, and S.L. Tabor, *Phys. Rev. C* **40**, 2028 (1989).
- [22] D.D. Caussyn, S.M. Aziz, P.D. Cottle, T. Glasmacher, and K.W. Kemper, *Phys. Rev. C* **40**, 2028 (1989).
- [23] L. Bargioni, P.G. Bizetti, A.M. Bizetti-Sona, D. Bazzacco, S. Lunardi, P. Pavan, C. Rossi-Alvarez, G. de Angelis, G. Maron, and J. Rico, *Phys. Rev. C* **51**, R1057 (1995).

- [24] J.K. Jewel, O.J. Tekyi-Mensah, P.D. Cottle, J. Döring, P.V. Green, J.W. Holcomb, G.D. Johns, T.D. Johnson, K.W. Kemper, P.L. Kerr, S.L. Tabor, P.C. Womble, and V.A. Wood, *Phys. Rev. C* **52**, (1995).
- [25] B. Myslek, B. Pietrzyk, Z. Sujkowski, and J. Szczepankowski, *Acta Phys. Pol. B* **2**, 441 (1971).
- [26] W. Urban, J.C. Bacelar, J.R. Jongman, R.F. Noorman, M.J.A. de Voigt, J. Nyberg, G. Sletten, M. Bergsröm, and H. Ryde, *Nucl. Phys.* **A578**, 204 (1994).